Application of On-line Impedance Measurement Using Fast Fourier Transform to Electrochemical Systems

Tetsuya Osaka* and Katsuhiko Naoi

Department of Applied Chemistry, School of Science and Engineering, Waseda University, Okubo, Shinjuku-ku, Tokyo 160

(Received April 15, 1981)

An on-line impedance measuring system based on the fast Fourier transform algorithm was constructed by application of only commercially available interfaces and the FORTRAN language available for an OKITAC System 50/10. A modification of the sampling system is effective for reducing two kinds of errors: the aliasing effect is greatly reduced because of the Nyquist frequency being doubled; the leakage effect is diminished because of the truncation interval being adjusted properly. The above modification enables us to acquire high-accuracy data with quite a small number of averagings processed during one measurement, that is, errors may greatly be reduced and the measurement time to get frequency spectra may be made extremely shorter. The modified impedance measurement using the FFT algorithm is applicable to electrochemical systems proceeding not only at a mercury electrode–solution interface but also at a solid electrode–solution interface.

Impedance (or admittance) methods, providing a powerful means for electrochemical analysis, have been made applicable to practical uses through the use of a.c. bridges and phase-sensitive devices with a support by analog cross-correlation techniques. Recently much effort has been devoted to developing automatic operation devices in order to improve accuracy and satisfy a necessity for simultaneous handling of many data points. A great deal of development has been made in impedance measurements by the introduction of the so-called Fourier and Hadamard transformation which have the multiplex advantage. Smith *et al.*[1] applied the multiplex technique using the FFT (fast Fourier transform) algorithm[2] to the electrochemical field and later Schwall *et al.*[3] extended the system so as to cover a wide frequency range from 10 Hz to 125 kHz. Multiplex techniques with construction of a pseudo-random noise spectrometer[4] using the Fourier transform algorithm and with establishment of a new digital signal processing method using the Hadamard transformation algorithm[5] have also been applied to the field of dielectric dispersion measurements. De Levie *et al.*[6] used a similar multiplex technique with sinusoidal wave collection signals in a biomembrane research and recently improved the impedance method in use in the electrochemical field by applying the digital synchronous detection using the Hadamard transformation algorithm.[7]

In this communication, we will try to take out the essential multiplex advantage by means of the modified FFT impedance measurement and to make it possible to acquire high accuracy from a short time measurement with a small number of averagings; we will also describe a simple system which can be composed only of commercially available interfaces without cumbersome hardware construction and which can be operated with the FORTRAN language available for the OKITAC System 50/10; finally, the system composed will be applied not only to mercury electrode–solution systems but also to solid electrode–solution systems.

Principle of Method

Every impedance method using various small-amplitude excitations essentially contains equivalent information as indicated in terms of mathematical transformation. The principle of this method in use in electrochemistry has been introduced.[1,8] The admittance $Y(\omega)$ of a linear or shift-invariant system is completely given by a cross-power spectrum between the excitation and response of the system as follows:

$$Y(\omega) = i(\omega)/e(\omega)$$
$$= i(\omega)e^*(\omega)/e(\omega)e^*(\omega),$$

where $e(\omega)$, $e^*(\omega)$, and $i(\omega)$ are a frequency domain spectrum of the applied potential, that of its complex conjugate, and that of faradaic current, respectively. This property of $Y(\omega)$ enables us to measure all frequency components simultaneously and to reduce the Fourier transformation to a demultiplexing process. Though in principle any excitation waveforms contain the same information, cross-power spectra in practical systems have to be obtained in a finite time, which requires the most suitable excitation waveform signal to be chosen. Therefore, the present system was designated to utilize the periodic pseudo-noise, which had been studied by Smith *et al.*[1] and Husimi *et al.*[4]

Instrumentation

Hardware Arrangement. The impedance measurement scheme was implemented on an OKITAC System 50/10 minicomputer (memory cycle time 0.65 μs, 75 kB) by using a floppy-disk-oriented system equipped with DMA interface cards. The maximum sampling rate of the system is 20 μs. The schematic diagram for the system is shown in Fig. 1. Programs and data are stored on floppy disks and output data may be displayed on an interfaced oscilloscope or X-Y plotter. Low pass filters are set up for three cut-off frequencies of 2.5, 7, and 12 kHz. The frequency range is restricted mainly by both the noise-applying rate $\Delta t'(f_{max}=(2\Delta t')^{-1})$ and the potentiostat response. The low pass filters (LPF) were built up by our laboratory (40 dB Butterworth) or by Fuso-Seisakusho (80 dB Butterworth), for cutting out the aliasing effect and smoothing computer-synthesized noises. The high pass filters (HPF), which were built

TABLE 1. RELATIONSHIP OF SAMPLING RATE WITH FREQUENCY LIMITS (MAXIMUM AND MINIMUM) AND MEASUREMENT DURATION IN THE CASE OF 1024-POINT (2^{10}) PSEUDO-NOISE

	Sampling rate $\Delta t/\mu s$	Noise-applying rate $\Delta t'/\mu s$	$f_{min}=(N\Delta t')^{-1}$ Hz	$f_{max}=(2\Delta t')^{-1}$ Hz	Measurement time $f_{min}^{-1}\times 3$/ms
System 1[a]	20	80	12.2	6250	245.8
	50	200	4.9	2500	614.4
	250	1000	1.0	500	3072.0
System 2[b]	20	40	24.4	12500	122.9
	50	100	9.8	5000	307.2
	250	500	2.0	1000	1536.0

a) System 1 means the system consisting of simultaneous sampling process of excitation $e(t)$ and response $i(t)$ (where the excitation and response are alternatively sampled with $\Delta t/\mu s$ interval and corrected with software technique). b) System 2 means the system consisting of separate sampling process of excitation $e(t)$ and response $i(t)$ (where the excitation is stored before measuring response).

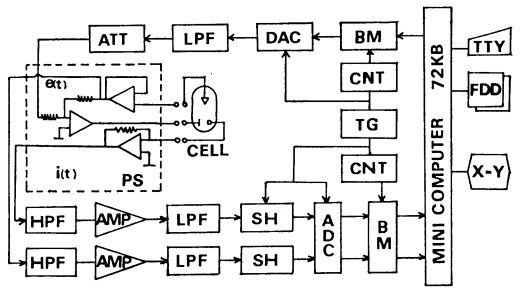

Fig. 1. Block diagram of FFT impedance instrument. Minicomputer: OKITAC system 50/10, DAC: digital-to-analog converter(12 bit), ADC: analog-to-digital converter(12 bit), TTY: teletypewriter, FDD: floppy disk drive assembly, X-Y: X-Y plotter, TG: timing generator, CNT: controller, BM: buffer memory, SH: sample and hold amplifier, LPF: low pass filter (cut off frequency 2.5, 7, 12 kHz), HPF: high pass filter (cut off frequency 1 Hz), ATT: attenuator, AMP: amplifier, PS: potentiostat.

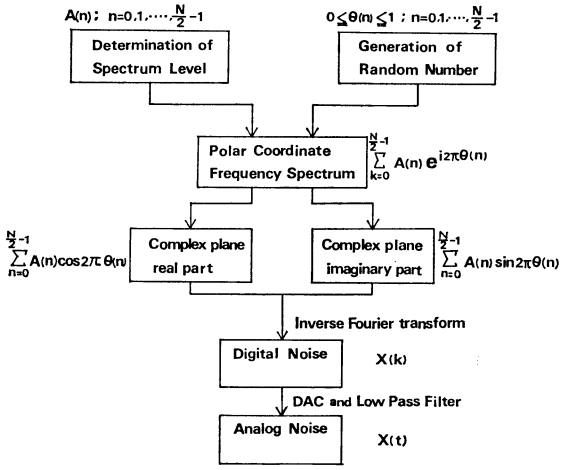

Fig. 2. Procedure for computerized digital wave form generation. $A(n)$: Amplitude array in frequency domain, $\theta(n)$: phase array in frequency domain, $\chi(k)$: digital time domain array, $\chi(t)$: analog time domain array.

by Fuso-Seisakusho, cut out dc and frequency components lower than 1 Hz. The potentiostat with high response (home built or Fuso-Seisakusho HOPATS-3)† was used instead of a dual-potentiostat as used by Smith *et al.*[1]

Generation of Pseudo-noise. Pseudo-noises generated by the minicomputer are subject to a synthesis as shown in Fig. 2. First, twenty frequency components are selected so as to avoid higher-harmonics (especially the second-harmonics). The phase component array is loaded with random numbers between 0 and 2π. The amplitudes of the selected frequency components are set as constant non-zero levels and those of the others as zero in order for all the frequency components to be at the same excitation energy. The "complex plane" frequency-domain array with 2048 points, which has been transformed from the "polar coordinate" frequency spectrum, is converted into the time-domain digital waveform with 1024 points by use of the inverse FFT. Real and imaginary components of the complex plane are to be set as even and odd functions, respectively, in order that time domain results may become of real function. The analog pseudo-noise thus arranged is applied ten times to the measuring cell to produce a periodic noise and steady-state response. Typical examples of frequency limits and measurement-time durations, as calculated from sampling rates, are listed in Table 1. Three kinds of sampling rates, *e.g.*, 20, 50, and 250 μs, lead to arrangement of three frequency ranges as shown in Table 1, thus allowing three frequency range measurements to provide high accuracy on wide frequency measurements. Since the measurement-time duration is equal to three times the reciprocal of f_{min} ($f_{min}=(N\Delta t')^{-1}$), the measurement time is dependent on the minimum frequency value.

Measuring System. The data acquisition and calculation processes for the transfer function are shown in Fig. 3. Two alternative sampling systems, Systems 1 and 2, are adopted. System 1, designed to perform simultaneous sampling of excitation $e(t)$ and response $i(t)$, samples both data alternately at $\Delta t/\mu s$ intervals and corrects them by the software technique based on the equation $Y(\omega)=Y'(\omega)e^{-i\omega\tau}$ (where Y, Y', and τ are the admittance of real response, that of delayed response, and the delay time Δt of sampling,

† The response rate is 2 μs under the conditions of 1:1 gain and 1 kΩ resistor.

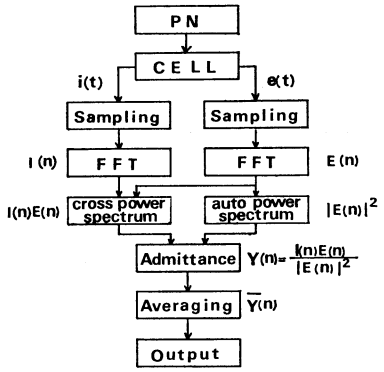

Fig. 3. Data acquisition and calculation processes for transfer function.

repectively). System 2, designed to store the excitation *e(t)* before response *i(t)* is measured, samples data of *e(t)* and *i(t)* separately. System 2 has two advantages over System 1: it can measure higher frequencies because it has its maximum frequency (f_{max}) doubled; it requires such a memory capacity as decreased to two thirds of that of System 1. We usually used System 2 because of these advantages. Data are acquired with 2048 points to be transformed into the frequency domain by means of the FFT. The transfer function of the measuring cell is calculated as admittance after the cross-power and auto-power spectra have been calculated. Final data of admittance are obtained after sampling and averaging which has been made of the last three waveform cycles of the ten-time-applied waveform signals. A remarkable feature of this sampling process is that the pseudo-noise output signal consisting of 1024 points is sampled at a doubled sampling rate (*viz.*, the noise is sampled with 2048 points). Since this sampling system causes the Nyquist frequency to be increased, errors due to the aliasing effect may be depressed (*cf.* Figs. 4 and 5). The leakage effect also may be made ineffective by adequate selection of the truncation interval which is equal to a multiple of the period. Thus, shorter-time measurement for frequency spectra may be realized by means of averaging the last three waveform signal responses.

Experimental

Polarographic measurements were performed on a Metrohm hanging mercury drop electrode (HMDE) with a surface area of 2.38×10^{-2} cm². Solutions for polarographic experiments on HMDE was purified with active charcoal after being prepared with reagent chemicals and triply-distilled water. For solid electrode–solution systems, smooth platinum (9.01×10^{-2} cm²) and gold (9.20×10^{-2} cm²) wire electrodes were used as working electrodes. To bring the solid-electrode surface into a reproducible condition, the working electrodes were cleaned with concentrated nitric acid and pretreated by allowing the electrode potentials to be scanned between the states of hydrogen and oxygen evolutions at 10 V s^{-1} for several tens of minutes. The silver–silver chloride or mercury–mercurous sulfate electrode was used as the reference electrode and the potentials were registered relative to the saturated calomel electrode (SCE). Experiments were performed in a purified nitrogen atmosphere at 25 °C.

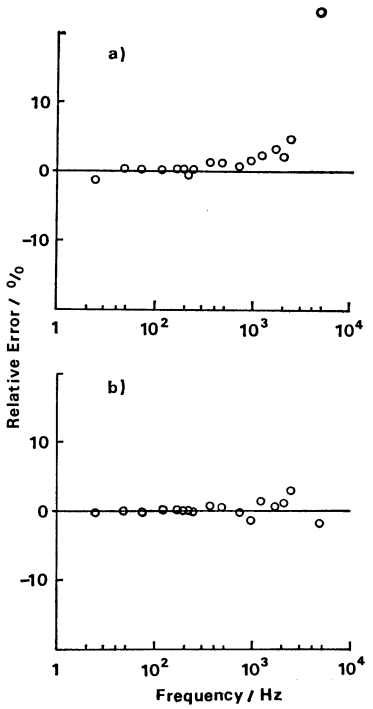

Fig. 4. Relative errors of power spectrum for System 2 using the same duration of sampling rate and noise-applying rate ($\Delta t=\Delta t'=120$ μs).
a): Relative error of power spectrum before passing LPF, b): relative error of power spectrum after passing LPF.

Results and Discussion

Dummy Cell Results. Figures 4(a) and (b) show typical data on relative errors for power spectra of pseudo-noise in the case where sampling rate is equal to the noise-applying rate ($\Delta t=\Delta t'=120$ μs); Figures 4(a) and (b) correspond to before- and after-passage through the low pass filter. Since the Nyquist frequency is *ca.* 4.2 kHz for this sampling rate, the aliasing effect at the high frequency edge is clearly observed as shown in Fig. 4(a). The aliasing effect at the high frequency edge can be cut out by the low pass filter as shown in Fig. 4(b); however, relative errors of several percents are still recognized. In the case of Fig. 5 where the sampling rate is twice as high as the noise-applying rate ($\Delta t=60$ μs, $\Delta t'=120$ μs), the Nyquist frequency is made doubled to 8.3 kHz and the aliasing effect cannot be recognized even in the absence of low pass filter as seen from Fig. 5(a). The relative errors for Fig. 5(a), which are less than 0.1%, are almost equal to those obtainable after the smoothing by means of low pass filter has been applied as seen from Fig. 5(b). Therefore, the sampling system described above is obviously effective for reducing relative errors, making it feasible to reduce the apparent measurement time. A comparison with respect to transfer function between theoretical and experimental values for a typical dummy cell shown in the figure is illustrated by use of the complex impedance representation, Z_{cell}, in Fig. 6. The experimental

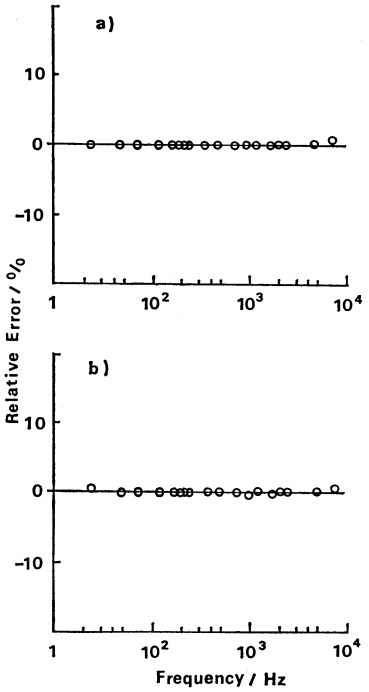

Fig. 5. Relative errors of power spectrum for System 2 using doubled sampling rate as compared with noise-applying rate (Δt=60 μs, $\Delta t'$=120 μs).
a): Relative error of power spectrum before passing LPF, b): relative error of power spectrum after passing LPF.

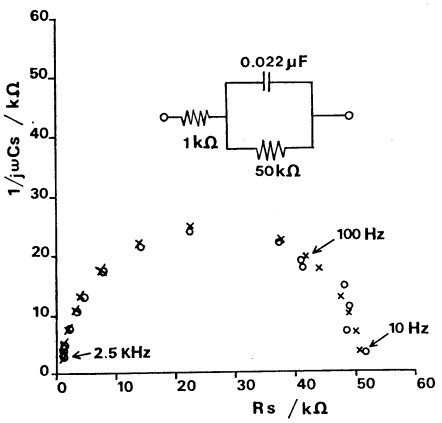

Fig. 6. Theoretical and experimental complex impedance representation of dummy cell shown in the figure.
×: Theoretical data, ○: experimental data.

data for the range from 10 Hz to 2.5 kHz are in fair agreement with the theoretical values at higher frequencies than 100 Hz. The data obtained at lower than 100 Hz, especially around 50 Hz, show some deviation from the theoretical data, which results from the line frequency interference.

Electrochemical Cell Results. An electrochemical system of a cadmium-ion reduction at an HMDE-acidified $ZnSO_4$ solution interface, which is the same system as Schwall *et al.*[3a,9] studied, was examined to obtain higher rate constants. The voltammogram for cadmium-ion reduction shown in Fig. 7(a) gives the maximum value of cot Φ (shown as $(\cot\Phi)_p$) at −0.557 V (SCE). Faradaic impedance representations as Z_k, after subtraction of solution resistance and double layer capacity, and plots of $(\cot\Phi)_p$ *vs.* $\omega^{1/2}$ at −0.557 V (SCE) are shown in Figs. 7(b) and (c). The slope for $(\cot\Phi)_p$ *vs.* $\omega^{1/2}$ plots yields the standard rate constant $k_c^\circ = 4.34\times10^{-2}$ cm s^{-1}, with the aid of the transfer coefficient α=0.35 given by Schwall *et al.*[3a,9] Though the value of k_c° obtained here is as small as half the values 8.7×10^{-2} and 8.5×10^{-2} cm s^{-1} obtained by Schwall *et al.*[3a,9] with and without scanning, respectively, our value may be considered to be in a reasonable range if data of other workers[10] are referred to.

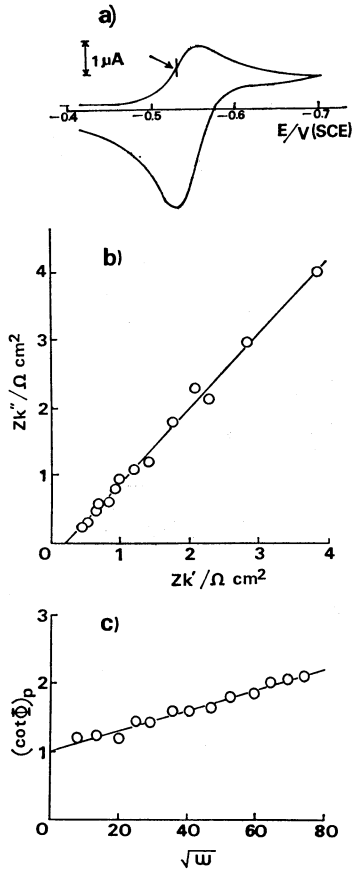

Fig. 7. Experimental results for cadmium ion reduction reaction on HMDE in 1.0 M zinc sulfate +0.18 M sulfuric acid (Cd^{2+} concentration=10^{-3} M), where M means mol dm^{-3}.
a): Single voltammogram of cadmium ion reduction, v=0.020 V s^{-1}, b): complex kinetic impedance representation of cadmium ion reduction at E=−0.557 V(SCE), c): relation between $(\cot\Phi)_p$ and $\omega^{1/2}$ of cadmium ion reduction at E=−0.557 V(SCE).

An electrochemical system of an adsorbed-hydrogen reaction at a platinum–sulfuric acid solution interface was examined as one of typical examples of solid electrode–solution systems. Figures 8(a) and (b) show typical cyclic voltammograms for reference and complex capacitance representations as $Y\omega^{-1}$ for the adsorbed-hydrogen region. The characteristic of complex capacitance representations is similar to that specified by one of the authors[11] using a phase-sensitive apparatus. The results are in accord with the equivalent circuit shown in the figure, previously proposed.[11]

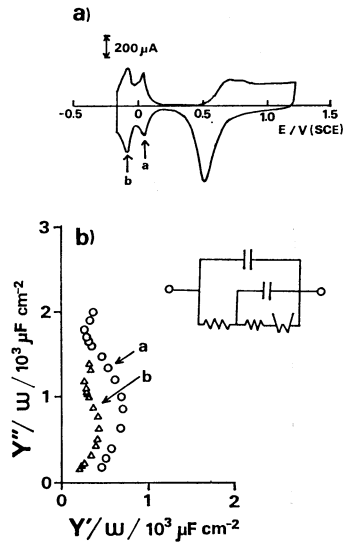

Fig. 8. Experimental results for adsorbed hydrogen reaction on platinum electrode in 0.5 M sulfuric acid.
a): Cyclic voltammogram of platinum electrode, v= 0.10 V s^{-1}, b): complex capacitance representation, $Y\omega^{-1}$, of adsorbed hydrogen reaction at 0.000 V (a) and −0.134 V(SCE) (b).

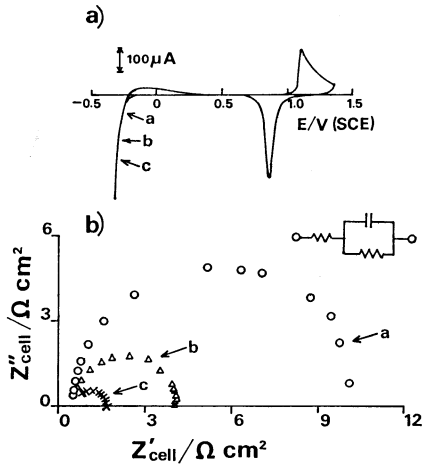

Fig. 9. Experimental results for hydrogen evolution reaction on gold electrode in 0.5 M sulfuric acid.
a): Cyclic voltammogram of gold electrode, v=0.10 V s^{-1}, b): complex impedance representation, Z_{cell}, of hydrogen evolution reaction at −0.374 V (a), −0.404 V (b), and −0.424 V(SCE) (c).

Another typical example of solid electrode-solution system, a hydrogen evolution reaction at a gold electrode–sulfuric acid solution interface, was also examined, data obtained being shown in Figs. 9(a) and (b). Figure 9(a) shows a typical cyclic voltammogram on a gold electrode and Figure 9(b) the complex cell impedance representation as Z_{cell} for the hydrogen evolution region. The characteristic of the complex cell impedance representation is of semicircle and in accord with the simple equivalent circuit shown in the figure, proposed by Masui and Ohashi.[12]

Therefore, the FFT impedance method described in the text may be concluded to be applicable to electrochemical systems proceeding not only at the mercury electrode–solution interface but also at the solid electrode–solution interface. Moreover, transient behaviors with time dependence, *e.g.*, variation in surface conditions with oxide formation, can be characterized by this method because of its short measurement time applicable.

The authors would like to thank Professor Emeritus Dr. Tadashi Yoshida, Waseda University, for his encouragement throughout this research, and Dr. Kazuhiko Nitadori, Systems Laboratory, OKI Electric Industry Company Ltd., for his valuable advice and discussion. T.O. would be greatful to Professor Dr. de Levie, Georgetown University, for calling his interest to the FFT impedance measurement. This work was partially supported by a Grant-in-Aid for Scientific Research from the Ministry of Education, Science and Culture.

References

1) D. E. Smith, *Crit. Rev. Anal. Chem.*, **2**, 247 (1971); S. C. Creason, J. W. Hayes, and D. E. Smith, *J. Electroanal. Chem.*, **47**, 9 (1973); S. C. Creason and D. E. Smith, *Anal. Chem.*, **45**, 2401 (1973).

2) E. O. Brigham, "The Fast Fourier Transform," Prentice-Hall, Inc., Englewood Cliffs, N. J. (1974).

3) a) R. J. Schwall, A. M. Bond, R. J. Loyd, J. G. Larsen, and D. E. Smith, *Anal. Chem.*, **49**, 1797 (1977); b) R. J. Schwall, A. M. Bond, and D. E. Smith, *ibid.*, **49**, 1805 (1977).

4) Y. Husimi and A. Wada, *Rev. Sci. Instrum.*, **47**, 213 (1976); H. Nakamura, Y. Husimi, and A. Wada, *J. Chem. Soc., Faraday Trans. 2*, **73**, 1178 (1977).

5) R. Hayakawa and Y. Wada, *IEE Conf. Publ.*, **177**, 396 (1979).

6) R. de Levie, J. W. Thomas, and K. M. Abbey, *J. Electroanal. Chem.*, **62**, 111 (1975).

7) P. F. Seeling and R. de Levie, *Anal. Chem.*, **52**, 1506 (1980).

8) "Computers in Chemistry and Instrumentation," ed by A. A. Pilla, J. S. Mattson, H. B. Mark, Jr., and H. D. Macdonald, Jr., Marcel Dekker (1972), Vol. 2, Chap. 6.

9) A. M. Bond, R. J. Schwall, and D. E. Smith, *J. Electroanal. Chem.*, **85**, 231 (1977).

10) S. Toshima, Y. Okinaka, and H. Okaniwa, *Denki Kagaku*, **31**, 854 (1963); J. K. Frishmann and A. Timnick, *Anal. Chem.*, **39**, 507 (1967); E. D. Moorhead and G. M. Frame, *J. Phys. Chem.*, **72**, 3684 (1968).

11) T. Osaka, Y. Sawada, T. Yoshida, and K. Nihei, *J. Electrochem. Soc.*, **123**, 1339 (1976).

12) M. Masui and K. Ohashi, Ex. Abstr. of the 47th Conf. Electrochem. Soc. Jpn., 1980, p. 102.